



EGCG-derived polymeric oxidation products enhance insulin sensitivity in db/db mice

Ximing Wu¹, Mingchuan Yang¹, Yufeng He, Fuming Wang, Yashuai Kong, Tie-Jun Ling, Jinsong Zhang*

Laboratory of Redox Biology, State Key Laboratory of Tea Plant Biology and Utilization, School of Tea & Food Science, Anhui Agricultural University, Hefei, 230036, China

ARTICLE INFO

Keywords:

Type 2 diabetes
Renin-angiotensin system
Insulin sensitivity
EGCG autoxidation Products
SELENOP
TXNIP

ABSTRACT

The present study investigated the influence of epigallocatechin-3-gallate (EGCG) and its autoxidation products on insulin sensitivity in db/db mice. Compared to EGCG, autoxidation products of EGCG alleviated diabetic symptoms by suppressing the deleterious renal axis of the renin-angiotensin system (RAS), activating the beneficial hepatic axis of RAS, and downregulating hepatic and renal SELENOP and TXNIP. A molecular weight fraction study demonstrated that polymeric oxidation products were of essential importance. The mechanism of action involved coating polymeric oxidation products on the cell surface to protect against cholesterol loading, which induces abnormal RAS. Moreover, polymeric oxidation products could regulate RAS and SELENOP at doses that were far below cytotoxicity. The proof-of-principal demonstrations of EGCG-derived polymeric oxidation products open a new avenue for discovering highly active polymeric oxidation products based on the oxidation of naturally occurring polyphenols to manage diabetes and other diseases involving abnormal RAS.

1. Introduction

Type 2 diabetes (T2D) is a metabolic disorder characterized by insulin resistance [1,2]. Previous studies have suggested that the dysfunction of the renin-angiotensin system (RAS) promotes insulin resistance [3–5]. Components of renin, angiotensin-converting enzyme (ACE), angiotensin-II (AngII), and AngII receptor type 1 (AT1R) have been strongly associated with glucose homeostasis impairment and diabetes [6–8], while pathways of ACE type 2 (ACE2)/angiotensin1-7 (Ang1-7)/Mas receptor (MasR) and AngII/AngII receptor type 2 (AT2R) have shown a beneficial role in T2D [6]. Thus, RAS modulation by inhibiting the deleterious axis and/or stimulating the beneficial axis has been suggested as a therapeutic strategy for T2D [6,9].

In addition to the RAS, selenocysteine-containing selenoprotein P (SELENOP) and thioredoxin interacting protein (TXNIP) have been

closely associated with insulin resistance. SELENOP, a liver-derived secretory protein, induces insulin resistance, upregulates glucose production, and causes hyperglycemia [10]. Its suppression represents a novel therapeutic strategy for T2D [10–12]. Metformin is a first-line medication for the treatment of T2D. Mechanistically, metformin suppresses hepatic expression and secretion of SELENOP [11,13]. Moreover, SELENOP-neutralizing antibodies have shown to be effective in improving insulin secretion and glucose sensitivity in T2D mouse models [14].

Furthermore, animal studies have shown that an overexpression of TXNIP induces pancreatic β -cell apoptosis and reduces insulin sensitivity in peripheral tissues, while its deficiency reduces insulin resistance and prevents T2D. Thus, TXNIP has been recommended as a novel therapeutic target of diabetes mellitus [15,16]. Moreover, TXNIP deficiency also reduces diabetic nephropathy [17]; thus, has been regarded as a

Abbreviations: ACE, Angiotensin-converting enzyme; AngII, Angiotensin-II; AT1R, AngII receptor type 1; ACE2, ACE type 2; Ang1-7, Angiotensin1-7; AT2R, AngII receptor type 2; Agt, angiotensinogen; AUC, Area under curve; ALT, Alanine aminotransferase; AST, Aspartate aminotransferase; BUN, Blood urea nitrogen; Cr, Creatinine; EGCG, Epigallocatechin gallate; EAOP, EGCG autoxidation products; EcSOD, Extracellular superoxide dismutase; GPx, Glutathione peroxidase; G6Pase- α , Glucose-6-phosphatase- α ; GLUT4, Glucose transporter 4; HOMA-IR, Homeostasis model assessment of insulin resistance; ITT, Insulin tolerance test; MasR, Mas receptor; MALDI-TOF-MS, Matrix-assisted laser desorption ionization-time of flight mass spectrometry; PBS, Phosphate buffer solution; PEPCK, Phosphoenolpyruvate carboxykinase; RAS, Renin-angiotensin system; T2D, type 2 diabetes; TXNIP, Thioredoxin interacting protein; Trx, Thioredoxin.

* Corresponding author.

E-mail address: zjs@ahau.edu.cn (J. Zhang).

¹ Contributed equally.

<https://doi.org/10.1016/j.redox.2022.102259>

Received 16 January 2022; Accepted 3 February 2022

Available online 9 February 2022

2213-2317/© 2022 The Authors.

Published by Elsevier B.V. This is an open access article under the CC BY-NC-ND license

(<http://creativecommons.org/licenses/by-nc-nd/4.0/>).

promising therapeutic drug target in diabetic nephropathy [18].

Epigallocatechin gallate (EGCG) is the most abundant catechin in green tea that possesses the highest anti-diabetic effect among various tea catechins [19]. Oral administration of EGCG or green tea polyphenol extracts, in which EGCG is a major functional ingredient, can prevent high-fat and/or high-fructose diet-induced insulin resistance in mice or rats [20–24]. Moreover, in db/db mice, EGCG increases HOMA-IR and serum insulin despite its dose-dependent decrease of fasting blood glucose [25,26].

EGCG undergoes autoxidation in neutral or alkaline pH

environments to form oligomeric and polymeric products referred to as EGCG autoxidation products (EAOP) [27,28]. Yet, it is well known that polyphenol polymers exhibit low or no oral bioavailability [29,30]. However, polyphenol polymers have been reported to have enhanced biological activities or chemical properties *in vitro*. For instance: 1) EAOP depletes cysteine [31] and inhibits lysozyme fibrillation [32] more efficiently than EGCG; 2) the brownies (polyphenol polymers) inhibits cancer cell proliferation more efficiently than green tea extract on the same weight basis [33]; 3) inhibitory effect on ACE activity is dependent on the number of epicatechin units in the procyanidin with

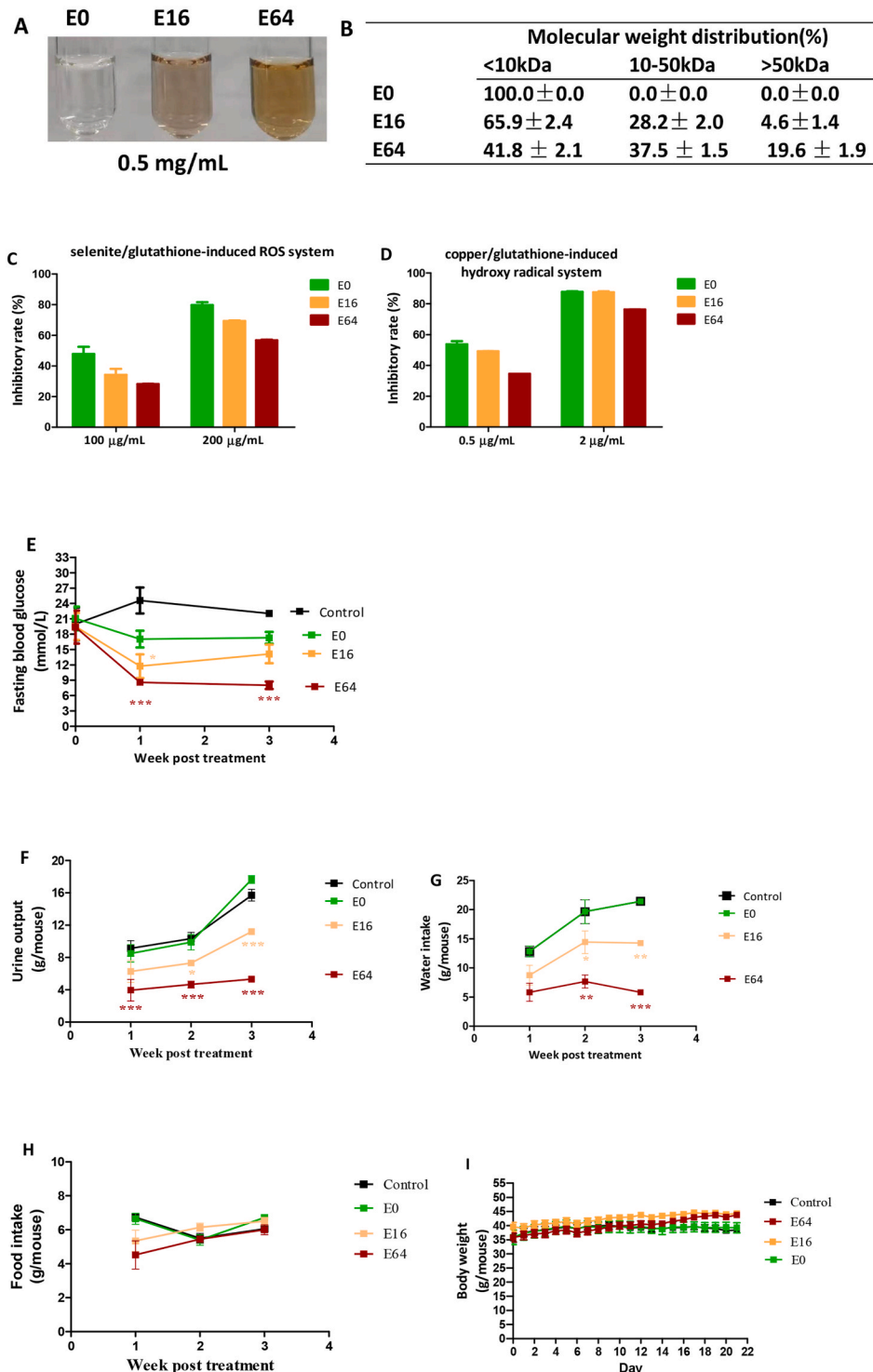


Fig. 1. *In vitro* characterization and *in vivo* hypoglycemic effect of EGCG and EAOP. (A–D) *In vitro* characterization. (A) color profile; (B) molecular weight distribution; (C) scavenging ROS in selenite/glutathione system; (D) scavenging hydroxyl radical in copper/glutathione system. Data are presented as the mean ± range (n = 2). (E–H) *In vivo* hypoglycemic effect. db/db mice (n = 6/group) were i.p. administered with E0 (EGCG), E16, and E64, respectively, at a dose of 10 mg/kg daily for three weeks. (E) Fasting blood glucose. (F) Urine output. (G) Water intake. (H) Food intake. (I) Body weight. Data are presented as the mean ± SEM. *P < 0.05, **P < 0.01 and ***P < 0.001, compared to the control.

tetramer/hexamer being more potent than monomer/dimer [34,35]; 4) procyanidins, oligomers, and polymers can inhibit esophageal adenocarcinoma cell proliferation *in vitro* [36]. Thus, we hypothesized that EAOP might exhibit biological activities *in vivo* provided it could be effectively delivered to tissues.

To avoid intestinal absorption barrier and degradation in the digestive system, several therapeutic drugs for diabetes such as insulin, amylin and dulaglutide are routinely administered [37,38]. The aim of this study was to investigate the potential role of EAOP on T2D model mice (db/db). EAOP was intraperitoneally (i.p.) injected. Our data showed that large molecular weight EAOP could efficiently ameliorate syndromes of T2D and increase insulin sensitivity by regulating RAS, SELENOP, and TXNIP.

2. Results

2.1. Preparation and therapeutic effect of EAOP

EGCG was dissolved in 0.2 M phosphate buffer solution (PBS, pH 8.0) at a concentration of 5 mg/mL. Autoxidation of EGCG was allowed to take place at 37 °C for 16 and 64 h. These samples were referred to as E16 and E64, respectively. Accordingly, EGCG immediately dissolved in the PBS was presented as E0. Brown color developed with autoxidation progress (Fig. 1A), suggesting that high molecular weight products gradually increased. Indeed, the >50 kDa fractions from E0, E16 and E64 were 0%, 4.6% and 19.6%, respectively, and the 10–50 kDa fraction from E0, E16 and E64 were 0%, 28.2% and 37.5%, respectively, as evaluated by ultrafiltration centrifugation with molecular weight cutoffs of 10 kDa and 50 kDa (Fig. 1B).

We next compared capacities of E0, E16, and E64 in scavenging reactive oxygen species (ROS). In a selenite/glutathione induced ROS model [39], ROS-scavenging potency was reduced in a time-dependent oxidation manner as expected; however, it is worth noting that 64-h oxidation only caused approximately 20% reduction (Fig. 1C). A similar decrease in antioxidant activity of EAOP was also observed in the copper/glutathione-induced hydroxyl radical model (Fig. 1D) [40]. These results demonstrated that E64 still possesses adequate antioxidant activity despite its pronounced oxidation.

E0, E16, and E64 were then i.p. injected into db/db mice (8 weeks of age) at a daily dose of 10 mg/kg for 3 consecutive weeks. The fasting blood glucose levels of the control group were over 20 mM during the experimental period. E0 did not show a significant anti-hyperglycemia effect. E16 only exhibited a transient anti-hyperglycemia effect, while E64 treatment significantly and persistently suppressed fasting blood glucose levels to less than 10 mM (Fig. 1E).

Hyperglycemia triggers osmotic diuresis, which is referred to as polyuria in diabetic subjects. The control group had high urine output levels (Fig. 1F); the urine output levels in db/db mice were the highest in E0 and the lowest in the E64 (E0 > E16 > E64) (Fig. 1F). As a compensatory response of polyuria, db/db mice normally consume large amounts of water, a phenomenon known as polydipsia. The influence of E0, E16, and E64 on hyperglycemia of db/db mice could be mirrored not only by polyuria reduction, but also by polydipsia reduction (Fig. 1G).

Neither body weight nor food intake was significantly affected by E0, E16, and E64 (Fig. 1H and I). Overall, E0 had no effect on diabetic symptoms, while E64 powerfully rectified abnormal symptoms of T2D; E16 was less effective.

2.2. The therapeutic effect of high-dose E16

Since the above experiment showed that E16 at the dose of 10 mg/kg (i.p.) had low therapeutic efficacy, we heightened its dose to 40 mg/kg (i.p.) to observe its therapeutic effect in db/db mice. For 4 consecutive days of treatment, E16 suppressed fasting blood glucose levels from 17.1 mM to 6.5 mM and reduced plasma insulin levels from 5.4 ng/mL to 1.2 ng/mL, resulting in great improvement of insulin sensitivity as

evidenced by a 91.2% reduction of HOMA-IR (Figs. S1A–C). As a result, hyperglycemia-triggered polyuria and the compensatory response polydipsia were rectified to nearly normal levels (Figs. S1D and S1E). The E16 treatment also reduced polyphagia and body weight (Figs. S1F and S1G). Moreover, E16 treatment downregulated renin, AngII, and AT1R and upregulated ACE2 in the liver (Fig. S2A), downregulated AT1R, and upregulated ACE2 in the kidney (Fig. S2B), and suppressed renal and serum ACE activity (Figs. S2C and S2D). These results suggest that E16 increases insulin sensitivity by activating the beneficial axis of RAS and inhibiting the deleterious axis of RAS.

2.3. The therapeutic effect of low-dose E64

Since the above experiment showed that E64 at the dose of 10 mg/kg (i.p.) exhibited high therapeutic efficacy, we performed a dose-dependent experiment to study the efficacy at a low dose in db/db mice. E64 was i.p. injected into db/db mice at a daily dose of 5 or 10 mg/kg for 3 consecutive weeks (referred to as E64-5 and E64-10, respectively). Reduced dose did not significantly compromise therapeutic efficacy as supported by the reduction in fasting blood glucose, plasma insulin, HOMA-IR (Fig. 2A–C). The insulin tolerance test (ITT) further suggested that the E64 treatment increased insulin sensitivity (Fig. 2D and E). In the most sensitive period to insulin administration (the first 60 min), fasting blood glucose levels of db/db mice were increased, whereas fasting blood glucose levels of db/db mice treated with E64 were decreased (Fig. 2D). Moreover, there were significant differences in fasting blood glucose levels between the control and E64 treatments at each examined time point (p all < 0.01) (Fig. 2D). Consequently, the area under curve (AUC) of ITT demonstrated that E64 markedly improved insulin intolerance compared to the control group (Fig. 2E). Also, the E64 treatments downregulated polyuria and polydipsia (Fig. 2F and G) without affecting polyphagia and body weight (Fig. 2H and I).

The similar therapeutic efficacy of the two doses was supported by their equivalent regulatory role on hepatic and renal RAS. In the liver, both doses upregulated the beneficial axis of RAS since ACE2 and AT2R protein expression, as well as ACE2 activity, were elevated (Fig. 3A and B). In the kidney, both doses showed dual regulation of RAS because ACE and AngII protein levels were decreased, and ACE2 activity was increased (Fig. 3C and D). These results suggest that E64, like high-dose E16, improves insulin sensitivity by activating the beneficial axis of RAS and inhibiting the deleterious axis of RAS.

2.4. Influence of E64 on SELENOP and TXNIP

Since E64 at two relatively low doses could effectively improve insulin sensitivity, we next sought to examine whether E64 also affects other well-documented targets associated with insulin sensitivity. In the liver, E64 suppressed SELENOP and TXNIP and inhibited glutathione peroxidase (GPx) activity (Fig. 4A and B). Probably as a result of hepatic TXNIP suppression, E64 increased hepatic thioredoxin (Trx) activity (Fig. 4C). In the kidney, E64 also suppressed SELENOP and TXNIP and increased Trx activity (Fig. 4D and E). Noteworthy, the higher dose of E64 was required for suppressing SELENOP in the liver (Fig. 4A) and the plasma (Fig. 4F) as well as TXNIP in the kidney (Fig. 4D), suggesting that the high-dose E64, in the long run, may gain a more reliable therapeutic efficacy. In support of this hypothesis, only high-dose E64 decreased renal gluconeogenesis and improved renal function (see below).

2.5. The therapeutic effect of different molecular weight fractions

E64 was separated into three molecular weight fractions (<10 kDa, 10–50 kDa, >50 kDa) through ultrafiltration centrifugation (Fig. 1B). The >50 kDa fraction exhibited dark brown color, whereas the other two fractions showed light brown color at a concentration of 1 mg/mL (Fig. 5A). Since E64 possesses antioxidant activities (Fig. 1C and D), we evaluated the antioxidant activities of the three fractions. In both the

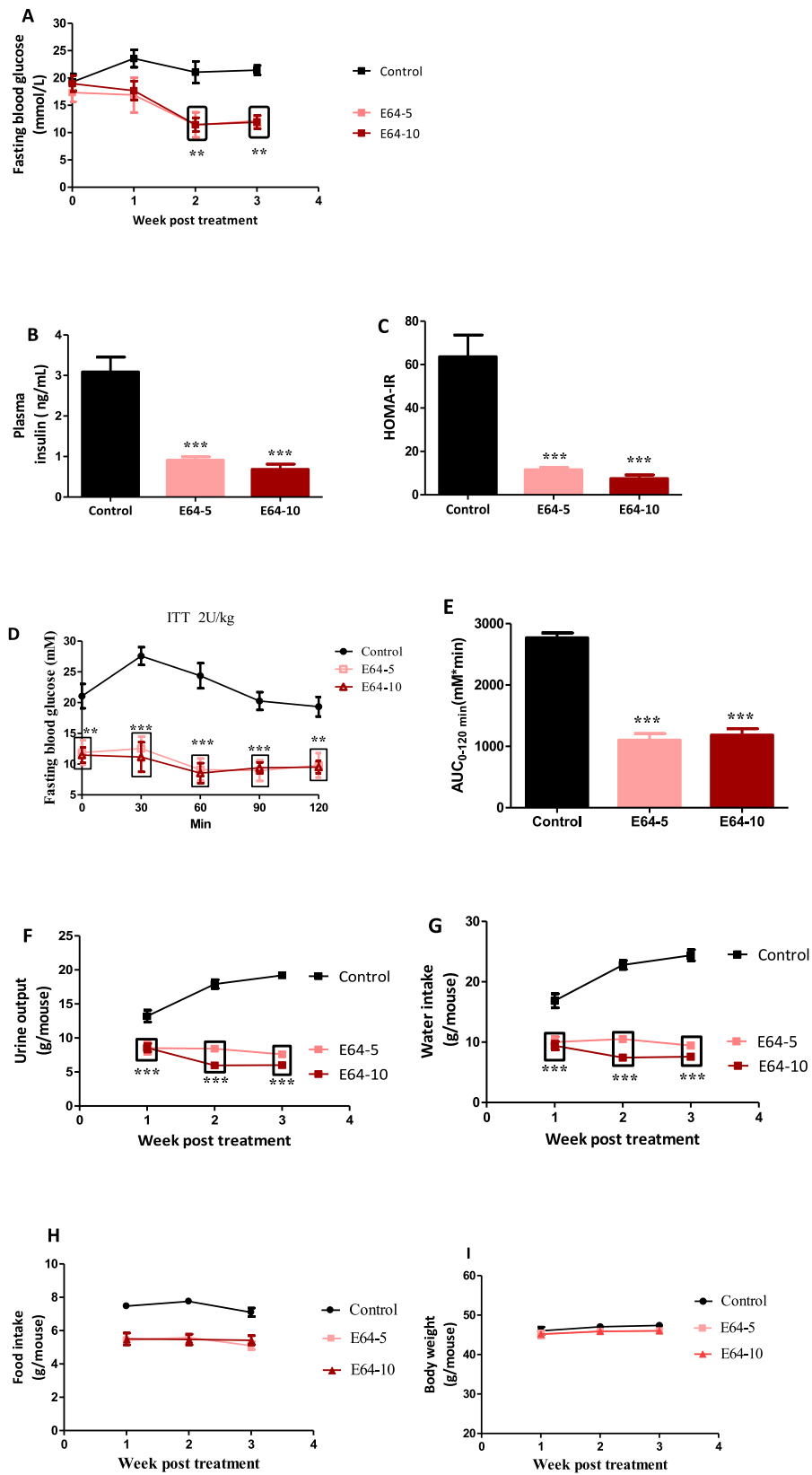


Fig. 2. Effects of E64 in db/db mice. db/db mice (n = 6/group) were i.p. administered with E64 at a dose of 5 or 10 mg/kg daily (referred to as E64-5 and E64-10, respectively) for three weeks. (A) Fasting blood glucose. (B) Plasma insulin. (C) HOMA-IR. (D) ITT. (E) ITT-AUC. (F) Urine output. (G) Water intake. (H) Food intake. (I) Body weight. Data are presented as the mean ± SEM. **P < 0.01 and ***P < 0.001, compared to the control.

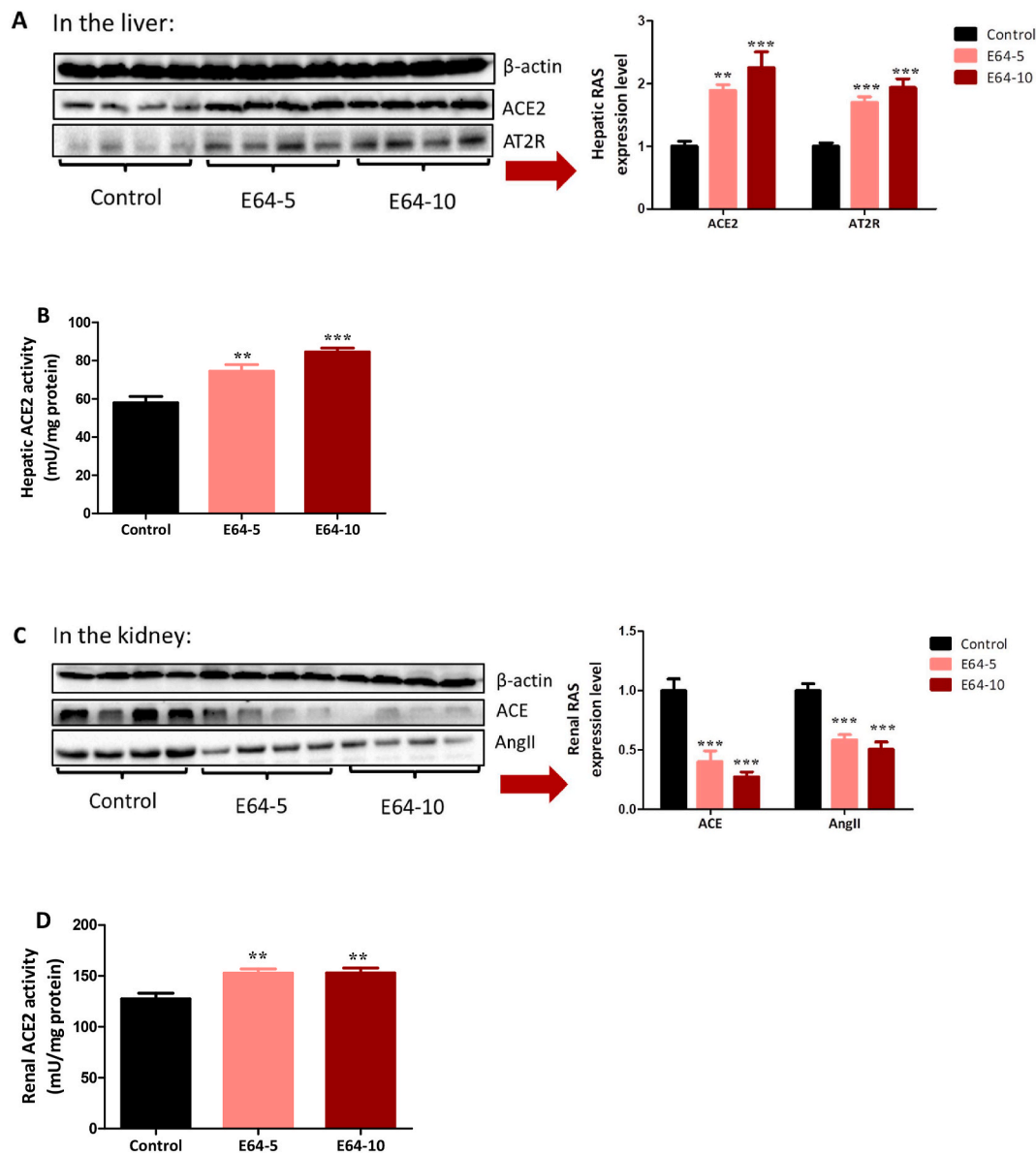


Fig. 3. Influence of E64 on hepatic and renal RAS. db/db mice ($n = 6/\text{group}$) were i.p. administered with E64 a dose of 5 or 10 mg/kg daily (referred to as E64-5 and E64-10, respectively) for three weeks. (A) Hepatic RAS. (B) Hepatic ACE2 activity. (C) Renal RAS. (D) Renal ACE2 activity. Data are presented as the mean \pm SEM. ** $P < 0.01$ and *** $P < 0.001$, compared to the control.

selenite/glutathione induced ROS model and copper/glutathione induced hydroxyl radical model, the three fractions exhibited similar antioxidant effects (Fig. 5B and C). These three fractions were i.p. injected into db/db mice at a daily dose of 5 mg/kg for 4 weeks. The <10 kDa fraction did not improve polyuria and polydipsia symptoms, while the other two fractions significantly ameliorated these symptoms in a molecular weight-dependent manner (Fig. 5D and E). None of these fractions significantly affected the body weight and food intake of the db/db mice (Fig. 5F and G). Only the >50 kDa fraction steadily controlled fasting blood glucose at nearly normal levels during the experimental period, while the <10 kDa fraction had no effect and the 10–50 kDa had intermittently anti-hyperglycemic effect (Fig. 5H). Thus, insulin level and HOMA-IR of the >50 kDa fraction-treated mice were further examined. All these parameters were significantly decreased ($p < 0.01$) (Fig. 5I and J).

To examine the response of local RAS to the treatment of the >50 kDa fraction, skeletal muscle, liver, kidney, abdominal adipose, and the pancreatic islet of each mouse were analyzed. The >50 kDa fraction

treatment activated the beneficial axis of RAS and/or inhibited the deleterious axis of RAS in examined tissues (Fig. 6A–E). Specifically, (i) components of the deleterious axis in the skeletal muscle (AT1R and rennin) were downregulated (Fig. 6A); (ii) in the liver, component of the deleterious axis (AT1R) was downregulated, and components of the beneficial axis (AT2R and ACE2) were upregulated (Fig. 6B); (iii) component of the deleterious axis (AT1R) was downregulated in the kidney (Fig. 6C); (iv) in the abdominal adipose, components of the deleterious axis (AT1R, renin, and AngII) were downregulated and a component of the beneficial axis (ACE2) was upregulated (Fig. 6D); (v) components of the beneficial axis (ACE2 and AT2R) were upregulated in the pancreatic islet (Fig. 6E). All these results suggest that the >50 kDa fraction improves insulin sensitivity by activating the beneficial axis of RAS and/or inhibiting the deleterious axis of RAS. Moreover, the >50 kDa fraction downregulated pancreatic SELENOP and TXNIP (Fig. 6F).

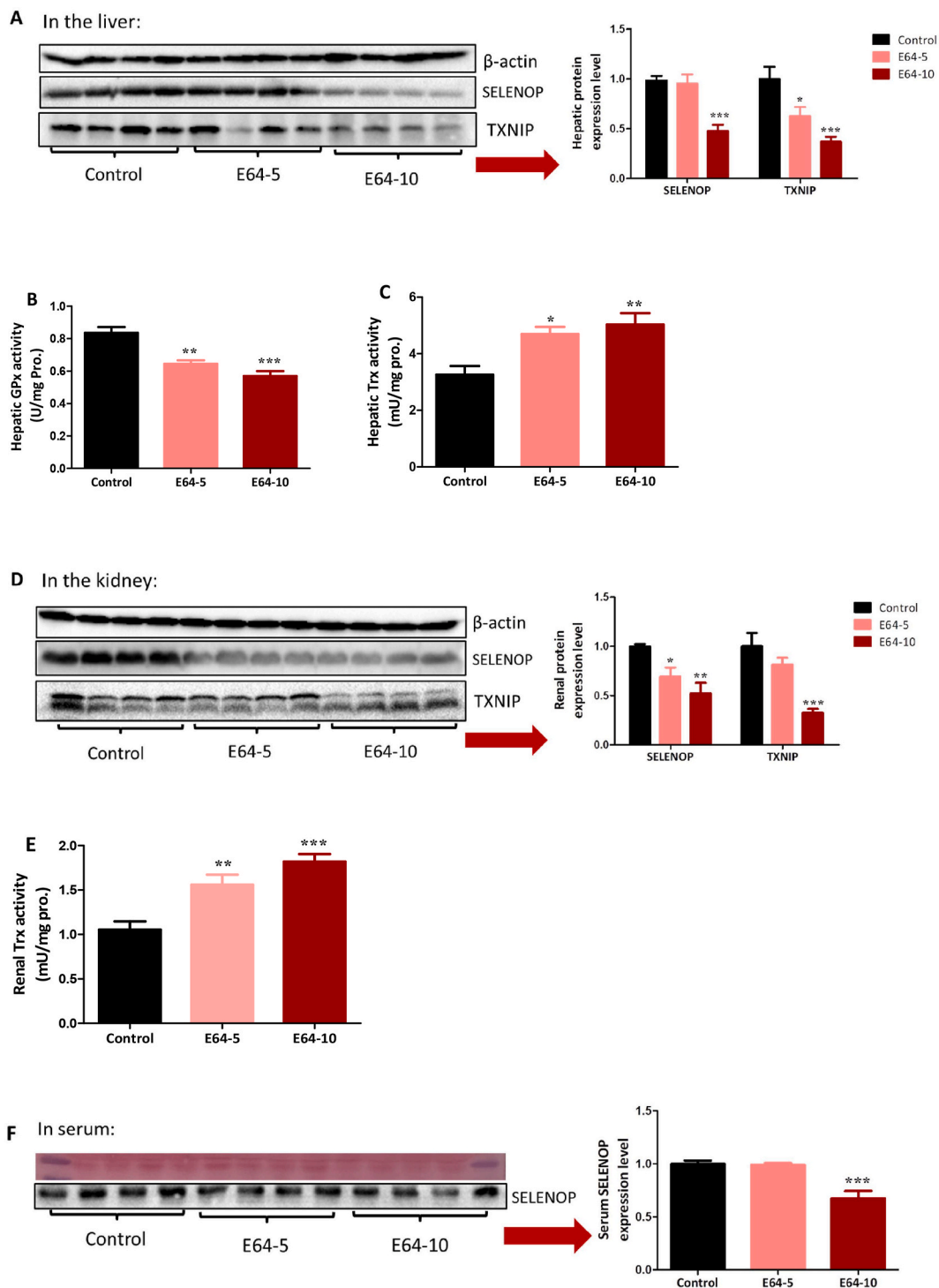


Fig. 4. E64 regulates multiple targets associated with insulin sensitivity. db/db mice ($n = 6/\text{group}$) were i.p. administered with E64 at a dose of 5 or 10 mg/kg daily (referred to as E64-5 and E64-10, respectively) for three weeks. (A) Hepatic SELENOP and TXNIP proteins. (B) Hepatic GPx activity. (C) Hepatic Trx activity. (D) Renal SELENOP and TXNIP proteins. (E) Renal Trx activity. (F) Serum SELENOP. Data are presented as the mean \pm SEM. * $P < 0.05$, ** $P < 0.01$ and *** $P < 0.001$, compared to the control.

2.6. Influence of EAOP on insulin sensitivity

Enhanced insulin sensitivity reduced gluconeogenesis in the liver and kidney and increased glucose transporter 4 (GLUT4) expression in the skeletal muscle and adipose tissue. Thus, we next examined the influence of the >50 kDa fraction on these biomarkers. The >50 kDa fraction suppressed renal and hepatic gluconeogenesis by down-regulating G6Pase- α and/or PEPCK (Fig. 7A and B), and increased

skeletal muscle and adipose tissue glucose uptake by upregulating GLUT4 (Fig. 7C and D), despite systemic insulin levels were only 47% of the control (Fig. 5I). The increased insulin responses in examined target organs under reduced insulin stimulation (as indicated by systemic insulin levels) suggested that the >50 kDa fraction increases insulin sensitivity.

Given that the kidney contributes approximately to 50% of the overall blood glucose by gluconeogenesis in T2D patients [41,42],

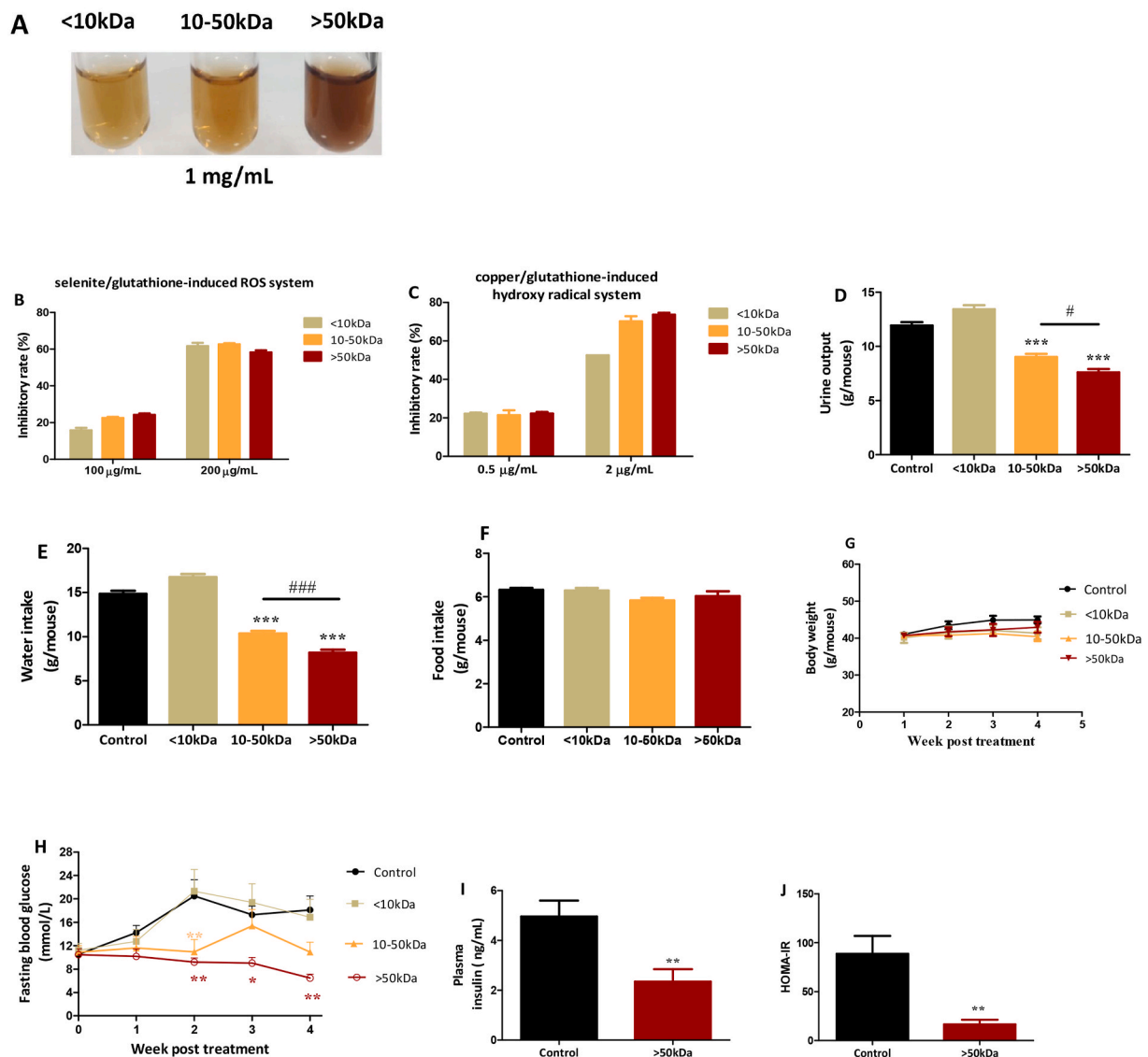


Fig. 5. *In vitro* characterization and *in vivo* hypoglycemic effect of different molecular weight fractions of E64. (A–C) *In vitro* characterization: (A) Color profile. (B) Scavenging ROS in selenite/glutathione system. (C) Scavenging hydroxyl radical in copper/glutathione system. Data are presented as the mean \pm range (n = 2). (D–J) *In vivo* hypoglycemic effect: db/db mice (n = 6/group) were i.p. administered with the three fractions of E64 (<10 kDa, 10–50 kDa, and >50 kDa) at a dose of 5 mg/kg daily for four weeks. (D) Urine output. (E) Water intake. (F) Food intake. (G) Body weight. (H) Fasting blood glucose. (I) Plasma insulin level. (J) HOMA-IR. Data are presented as the mean \pm SEM. *P < 0.05, **P < 0.01 and ***P < 0.001, compared to the control.

inhibiting renal gluconeogenesis by the >50 kDa fraction is potentially an important finding for T2D treatment. Thus, we revisited the influence of E64, which contains a relatively high percentage of the >50 kDa fraction on renal gluconeogenesis. Consistently, E64 (10 mg/kg, i.p.) significantly suppressed G6Pase- α (Fig. S3A) despite systemic insulin levels being only 22% of the control (Fig. 2B). Furthermore, we found that the reduced insulin stimulation on the kidney due to largely low systemic insulin levels did not compromise renal PI3K and AKT signal pathway (Fig. S3B), thus suggesting that insulin had a high regulative role.

2.7. Effects of EAOP on hepatic and renal functions

E16 significantly improved hepatic function but did not affect renal function (Table S1). Also, high-dose E64 and the >50 kDa fraction significantly improved renal function but did not affect hepatic function (Tables S2 and S3). Together, these results showed that EAOP was less likely to impair hepatic and renal functions. In contrast, they were more likely to improve hepatic and renal functions in individuals with T2D.

2.8. Delineation of EAOP influence on RAS in HepG2 cells

The above experiments showed that EAOP improved diabetic symptoms in db/db mice in an EGCG oxidation degree-dependent manner and an EAOP molecular weight-associated fashion. Moreover, we found that both high oxidation degree EAOP (E64) and high molecular weight EAOP (the >50 kDa fraction from E64) regulated RAS. Subsequently, we wanted to delineate EGCG oxidation degree-dependent and EAOP molecular weight-associated influences on RAS. For this purpose, HepG2 cells (human hepatic carcinoma cells with abnormal RAS) were employed. E64 downregulated renin and AngII while E16 and E0 had no effect at 20 μ g/mL (Fig. S4A). E16 was more efficient than E0 in suppressing renin and AngII at 40 μ g/mL (Fig. S4B). These results suggest that EGCG influences RAS in an oxidation degree-dependent manner.

As expected, the three fractions (<10 kDa, 10–50 kDa, and >50 kDa) showed molecular weight-associated influences on renin and AngII at either 5 μ g/mL (Fig. S5A) or 10 μ g/mL (Fig. S5B). Additional experiments were performed to investigate whether the >50 kDa fraction

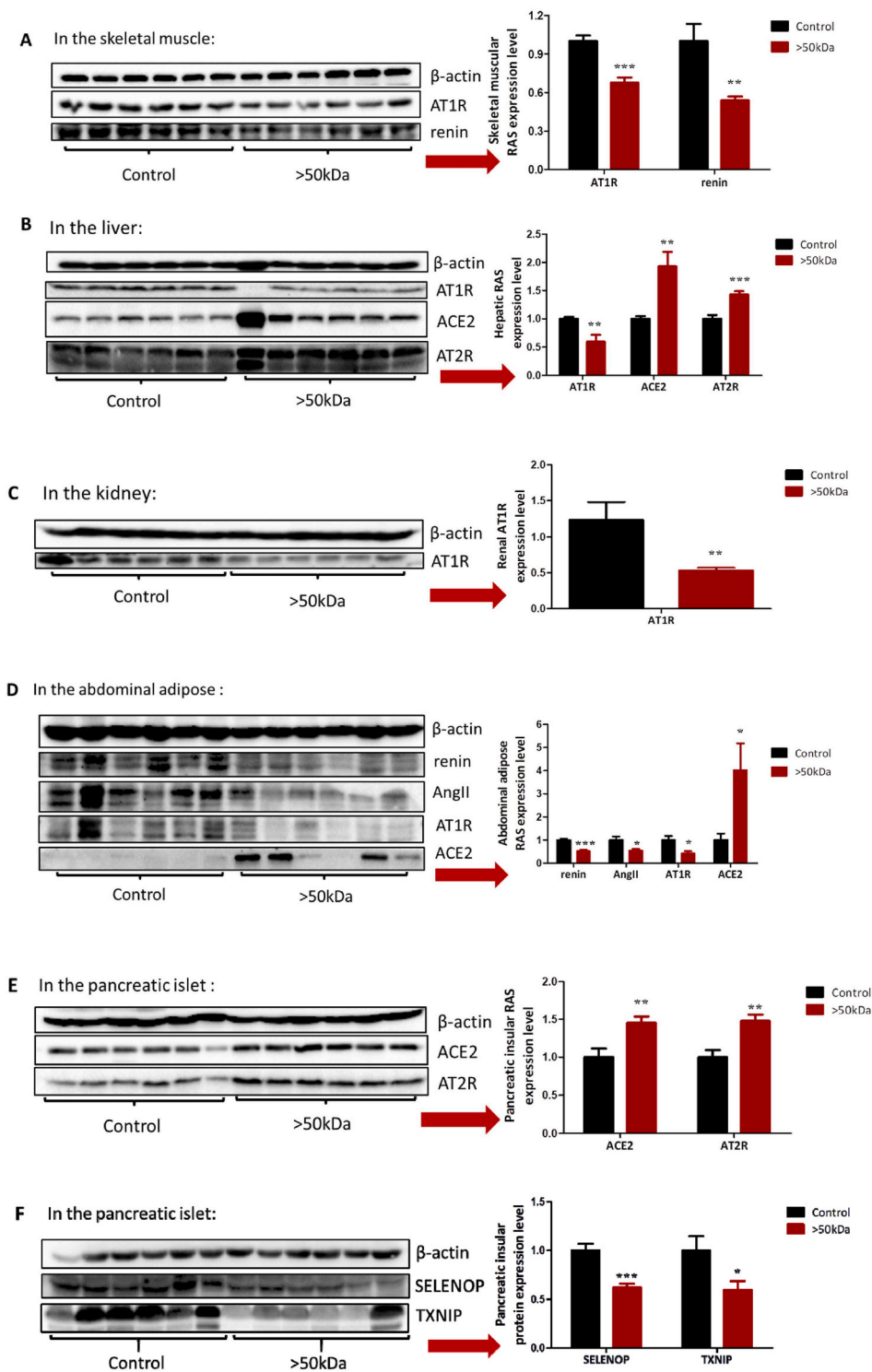


Fig. 6. Influence of the >50 kDa fraction on RAS, SELENOP, and TXNIP. db/db mice (n = 6/group) were i.p. administered with the >50 kDa fraction at a dose of 5 mg/kg daily for four weeks. (A) Skeletal muscular RAS. (B) Hepatic RAS. (C) Renal RAS. (D) Abdominal adipose RAS. (E) Pancreatic RAS. (F) Pancreatic SELENOP and TXNIP. Data are presented as the mean \pm SEM. *P < 0.05, **P < 0.01 and ***P < 0.001, compared to the control.

affects SELENOP and TXNIP in HepG2 cells. The >50 kDa fraction suppressed SELENOP (Fig. S5C) but not TXNIP (data not shown). Concerning cytotoxicity, half-maximal cytotoxic concentration (CC50) of E64 was 144 μ g/mL (Fig. S6A), and the >50 kDa fraction did not trigger cytotoxicity even at 320 μ g/mL (Fig. S6B). These results demonstrate that the >50 kDa fraction could generate an impact on RAS or SELENOP at doses far below toxic levels.

2.9. Tissue and cell coating of EAOP

We found that the >50 kDa fraction was coated on tissues such as the abdominal adipose following i.p. treatment of db/db mice for one month. Abdominal adipose exhibited brown color, which was in sharp contrast to tissue color in db/db mice treated with the PBS (Fig. S7A). The short-term but high-dose experiments using either the >50 kDa fraction or E64 in Kunming mice further validated this finding (Figs. S7B

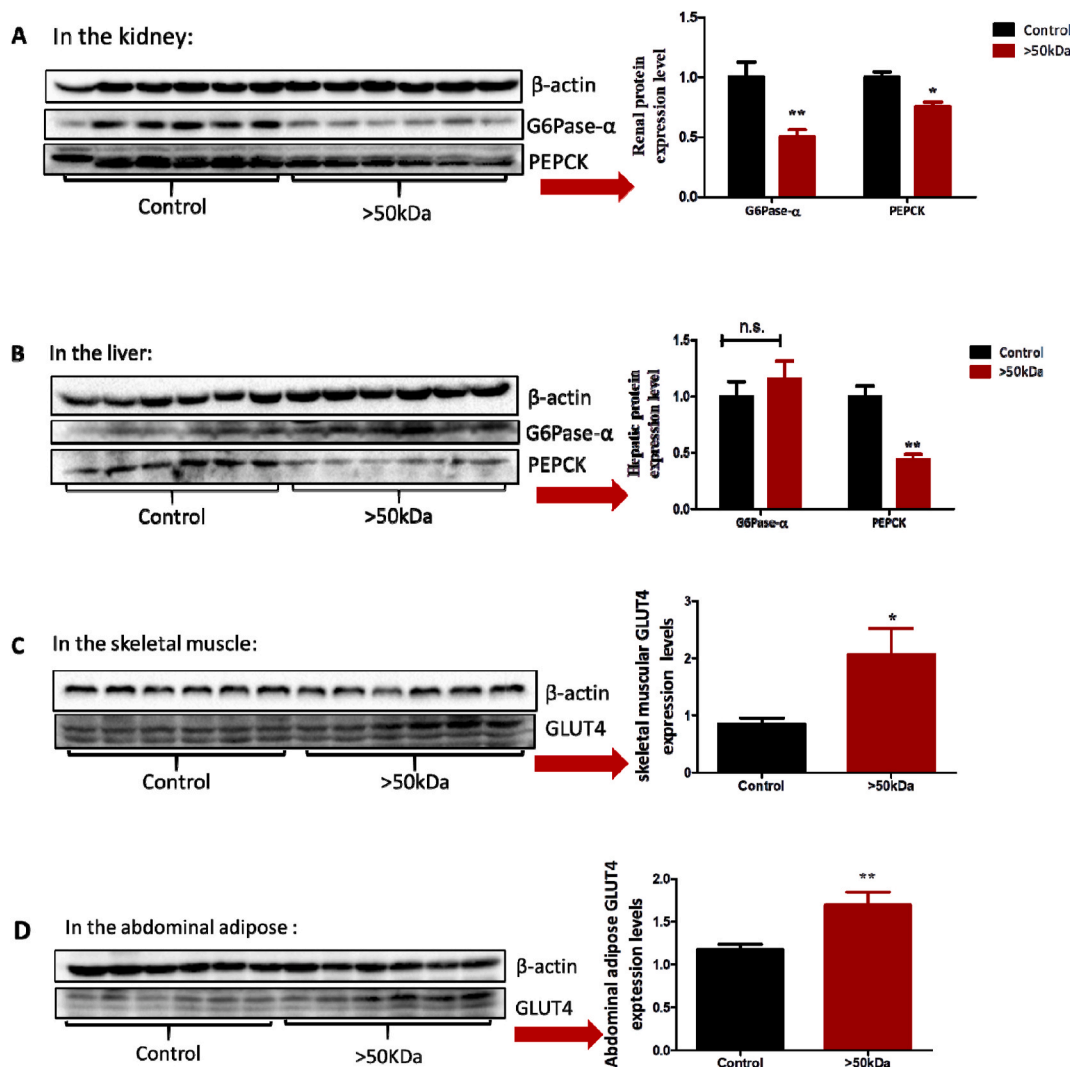


Fig. 7. Influence of the >50 kDa fraction on gluconeogenesis and GLUT4. db/db mice (n = 6/group) were i.p. administered with the >50 kDa fraction at a dose of 5 mg/kg daily for four weeks. (A) Renal G6Pase- α and PEPCK. (B) Hepatic G6Pase- α and PEPCK. (C) Skeletal, muscular GLUT4. (D) Abdominal adipose GLUT4. Data are presented as the mean \pm SEM. *P < 0.05, **P < 0.01 and ***P < 0.001, compared to the control.

and S7C). Similarly, cultured HepG2 also showed brown color after incubation with the >50 kDa fraction (Figs. S8A–a). To dissect cellular distribution of brown color, HepG2 cells were lysed. Only the sediment but not the supernatant exhibited brown color following the lysis centrifugation (Figs. S8A–b), implying that brown polymeric oxidation products probably stayed on the cellular surface. To test this hypothesis, the lysis of non-treated HepG2 cells was added with the >50 kDa fraction to observe the distribution of brown color following centrifugation, as shown in Figs. S8B–a. Only the supernatant but not the sediment exhibited brown color, whereas the addition of the >50 kDa fraction in non-treated HepG2 cells immediately prior to lysis resulted in the contrast distribution of brown color (Figs. S8B–b), being identical to the distribution profile as seen from HepG2 cells cultured in the presence of the >50 kDa fraction (Figs. S8A–b). These lines of evidence demonstrate that the >50 kDa fraction cannot penetrate into the cells and that it is coated on tissue or cellular surface.

2.10. Influence of EAOP on cholesterol-induced abnormal RAS

Obesity has been associated with cholesterol accumulation, and a high-fat diet or cholesterol loading has been reported to cause abnormal RAS expression [43,44]. We hypothesized that regulatory role on RAS by the >50 kDa fraction in obese db/db mice probably involves the

suppressive role of the >50 kDa fraction on cholesterol-stimulating abnormal RAS. In human renal proximal tubular epithelial cells (HK-2 cells), cholesterol plus 25-hydroxycholesterol increased protein expression of angiotensinogen (Agt), renin, and AT1R, while the >50 kDa fraction effectively protected against these increases (Fig. 8A). Surprisingly, the high dose (20 μ g/mL) pronouncedly reduced these proteins (Fig. 8A). Such a dramatic suppression to nonphysiological levels should be avoided by lowering dosage; however, it reinforces the concept that the surface coating of the >50 kDa fraction, as supported by the brown sediment following HK-2 cell lysis and centrifugation (Fig. 8B), is a highly effective approach for modulating RAS.

Next, we examined the cytotoxicity of the >50 kDa fraction in both untreated and high cholesterol-treated HK-2 cells. The results showed that the >50 kDa fraction did not trigger cytotoxicity even at 160 μ g/mL (Figs. S9A and S9B). These results demonstrate that the >50 kDa fraction could impact RAS at doses far below toxic levels.

2.11. Chemical entities of the >50 kDa fraction

We attempted to comprehend chemical entities in the >50 kDa fraction from E64 since this fraction exhibited the most effective improvement on diabetic symptoms in db/db mice and the highest regulatory role on RAS in HepG2 cells. By using matrix-assisted laser

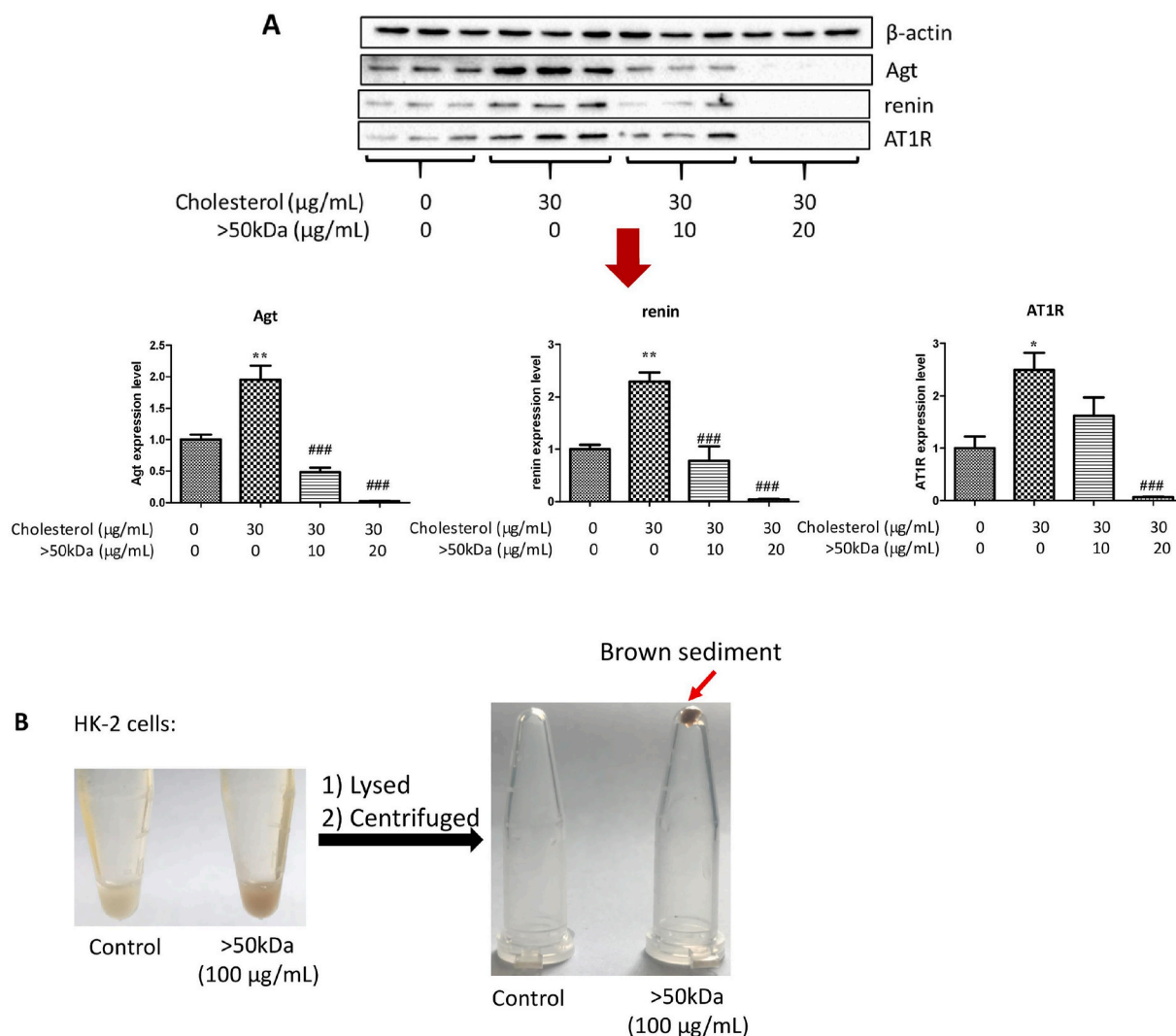


Fig. 8. Influence of the >50 kDa fraction on abnormal RAS induced by cholesterol in HK-2 cells. **(A)** Dose-dependent RAS regulation. Data are presented as the mean \pm SEM ($n = 3$). ** $P < 0.01$, compared to the control. # $P < 0.05$, ## $P < 0.01$ and ### $P < 0.001$, compared to cholesterol treatment. **(B)** Coating characterization. HK-2 cells were treated with the >50 kDa fraction (100 $\mu\text{g/mL}$) for 24 h, then the cells were lysed on ice for 3 min and centrifuged at 10,000 g for 5 min.

desorption ionization-time of flight mass spectrometry (MALDI-TOF-MS) with α -cyano-4-hydroxycinnamic acid (HCCA) as a matrix, tannic acid as a positive reference generated expected MS signals. Under the circumstance, the >50 kDa fraction did not show any MS signals (Fig. S10). Such an unsuccessful experiment is reminiscent of thearubigins, the most abundant oxidation product of tea catechins in black tea. Thearubigins are assumed to contain mammoth polymeric species (up to 30000) [28] with a molecular weight distribution from 2 kDa to 40 kDa [45,46]. However, due to the highly complex nature, there is still no evidence on the exact chemical structure of each component in the arubigins, despite the use of various sophisticated MS technologies such as MALDI-TOF-MS ESI-TOF-MS, ESI-FT-ICR-MS, and ESI-ion trap MS [47].

3. Discussion

EGCG has diverse biological activities. The existing consensus is that the redox-active EGCG should be maintained in non-oxidized status for achieving better biological functions. Yet, in this study, we found that EAOP was more efficient than EGCG in improving diabetic symptoms. The major active ingredients of E64 are located in the >50 kDa fraction. Yet, a crucial question is how this fraction, apparently unable to penetrate into cells due to high molecular weight, triggers anti-

hyperglycemia response in db/db mice. A previous study suggested that a delivery route of the >50 kDa fraction from the peritoneal cavity to various tissues is most likely through lymphatic ducts [48]. In this study, we found that the >50 kDa fraction was coated on tissues such as the abdominal adipose following one-month i.p. treatment in db/db mice, which is not consistent with the general consensus suggesting that the >50 kDa fraction is unlikely to enter into cells. Coating tannic acid on pancreatic islet surface with the aid of a biocompatible polymer *in vitro* improves islet functions after the pancreatic islet is transplanted into diabetic mice, leading to increased insulin sensitivity and euglycemia compared to uncoated control [49,50]. These studies foster the concept that extracellular antioxidant coating is probably a novel strategy for the management of diabetes. In supporting this concept, extracellular superoxide dismutase (EcsOD) has an important role in protecting against diabetes-related oxidative stress [51,52] and in improving diabetic complications such as albuminuria [53], nephropathy [54], cardiovascular disease [55], and retinopathy [56]. Like EGCG, the >50 kDa fraction also exhibits antioxidant traits. Unlike EGCG, which cannot be effectively coated on tissues *in vivo* because EGCG can enter into cells due to its low molecular weight, the >50 kDa fraction could be used for tissue coating of macromolecular antioxidants *in vivo*. Therefore, the >50 kDa fraction may act as an extracellular antioxidant, like EcsOD and coated tannic acid.

A closely related question is why E64, especially the >50 kDa fraction, improves fasting blood glucose levels in db/db mice. We found that both E64 and the >50 kDa fraction could regulate RAS by favoring insulin sensitivity via activating the beneficial axis of RAS and/or suppressing the deleterious axis of RAS in all examined tissues. Moreover, E64 downregulated hepatic and renal SELENOP and TXNIP, while the >50 kDa fraction suppressed pancreatic islet TXNIP and renal PEPCK/G6Pase- α . These additional actions are helpful for improving insulin sensitivity or reducing glucose production. However, a challenging question is how extracellular macromolecules like the >50 kDa fraction with antioxidant activity mediate these anti-hyperglycemic molecular responses. We speculated that at least two scenarios might be involved: (i) the beneficial result may resemble an episode of EcSOD and could be considered an overall improvement on oxidative stress and cell physiology; (ii) based on current *in vitro* finding in HK-2 cells, extracellular coating of high molecular weight EAOP could prevent against high cholesterol challenge, which induces abnormal RAS. Given obese db/db mice have a high level of deposition of tissue cholesterol and abnormal RAS, as well as significant regulatory effects of E64 or the >50 kDa fraction on abnormal RAS in db/db mice, the second hypothesis appears to be more mechanism-relevant. Despite detailed mechanism actions that should be elaborated in future studies, the influences of EAOP on RAS, SELENOP, TXNIP and/or PEPCK/G6Pase- α can explicitly explain why EAOP increases insulin sensitivity and reduces hyperglycemia in db/db mice.

We observed a significant influence of EAOP on RAS in each db/db mouse experiment independently using the >50 kDa fraction, E64, or E16. EAOP upregulated the beneficial axis of RAS and downregulated its deleterious axis in the same tissue. We also found that EAOP could upregulate the beneficial axis of RAS in one tissue and downregulate the deleterious axis of RAS in another one, which suggests that EAOP act as a dual regulator of RAS. Besides, the dual regulatory role could occur in multiple tissues (the liver, kidney, skeletal muscle, adipose tissue, and pancreatic islet) and in diverse components of the RAS (downregulation of renin, ACE, AngII, or AT1R of the deleterious axis, upregulation of AT2R, ACE2 or MasR of the beneficial axis). Thus, EAOP could be considered as a comprehensive regulator of RAS elements.

Nonetheless, the powerful effect of E64 in improving insulin resistance cannot be only ascribed to the regulatory role on RAS. E64 can modulate other pathways associated with insulin sensitivity to work in harmony with RAS regulation. Intriguingly, E64 suppresses two well-characterized selenoproteins in the liver, specifically SELENOP expression and GPx activity. In addition, E64 suppresses hepatic TXNIP and, as a result, increases hepatic Trx activity. These influences exerted by E64 could also be observed from the kidney, except GPx activity. As introduced in the previous section, SELENOP or TXNIP induces insulin resistance, and their suppression represents a novel therapeutic strategy for T2D [10–12,14–18]. The suppressive role of E64 on hepatic or renal SELENOP and TXNIP should participate in increasing insulin sensitivity. GPx modulates redox signaling pathways associated with insulin biosynthesis and insulin receptor activity [57]. Global overexpression of GPx leads to obesity and insulin resistance in mice [58]. The inhibitory role of E64 on hepatic GPx activity may also provide support for enhanced insulin sensitivity.

We also found that >50 kDa fraction can regulate RAS in multiple tissues vital for glucose utilization and glucose or insulin biosynthesis (the skeletal muscle, adipose tissue, liver, kidney, and pancreatic islet). Abnormal RAS increases insulin resistance in the skeletal muscle [5,59], adipose tissue [60], and liver [61,62]. Moreover, abnormal RAS in the kidney increases the progression of diabetic nephropathy towards end-stage renal disease in patients with T2D [63,64], while abnormal RAS in the pancreatic islets reduces islet blood flow and insulin biosynthesis, impairs β -cell secretory function and cell mass, and increases oxidative stress, inflammation, apoptosis, and fibrosis of the tissue [65–68]. The simultaneously systematic rectification of disordered RAS by the >50 kDa fraction is expected to generate a synergistic

role in enhancing insulin sensitivity and improving diabetic symptoms and complications. Nonetheless, the anti-diabetic mechanism of the >50 kDa fraction cannot only be ascribed to systematically dual regulation on the deleterious and/or beneficial axis of RAS. The >50 kDa fraction suppresses pancreatic islet TXNIP, which belongs to the top glucose-induced gene in the human islet [69]. TXNIP inhibition by the >50 kDa fraction should improve islet function since elevated TXNIP induces oxidative stress, promotes β -cell apoptosis, impairs β -cell function, and reduces insulin production [69,70]. This study found that the >50 kDa fraction also suppresses SELENOP in the pancreatic islet. It has been shown that excessive amounts of SELENOP impair the function of pancreatic β -cells and decrease pancreatic insulin levels and insulin secretion [14]; thus, pancreatic SELENOP inhibition by the >50 kDa fraction should help improve islet function. In addition, the >50 kDa fraction also inhibited renal PEPCK and G6Pase- α . Under the pathological condition of hyperglycemia, the handling of glucose by the kidney is altered; consequently, the kidneys contribute to approximately 50% of the overall blood glucose in T2D patients [41,42]. Like the liver, the increased glucose release by the kidney under the fasting state is due to gluconeogenesis [41,42]; thus, the downregulation of renal PEPCK and G6Pase- α proteins by the >50 kDa fraction should participate in reducing hyperglycemia.

4. Conclusion

Our data suggest that i.p. administration of EAOP is much more effective than EGCG in improving T2D symptoms in db/db mice. The pharmacological effects of EAOP are molecular weight-dependent, with high molecular weight fraction being more efficient. EAOP exerts an anti-hyperglycemic effect by a coating of EGCG-derived polymeric oxidation products on tissues, leading to activation of the beneficial axis of RAS and suppression of the deleterious axis of RAS, SELENOP, TXNIP, or renal PEPCK/G6Pase- α . The proof-of-principle demonstration of EGCG-derived polymeric oxidation products suggests that numerous polyphenol oxidation products, which could be conveniently prepared from diverse naturally occurring polyphenols under various oxidation conditions, are rich resources for discovering robust RAS regulator and anti-diabetic drugs.

5. Materials and methods

5.1. Reagents

EGCG (>99% purity) was purchased from Yibei Tea Technology, Inc. (Hangzhou, P.R. China). ACE and ACE2 activity assay kits were bought from BioVision Inc. (San Francisco, CA, USA). The primary antibodies against G6Pase- α , PEPCK, SELENOP, and GLUT4 were purchased from Santa Cruz Biotechnology (Dallas, TX, USA); primary antibodies against renin, AngII, ACE, ACE2, AT1R, AT2R, MasR, and Agt were obtained from Abcam (Cambridge, UK); primary antibodies against β -actin, TXNIP, PI3K, p-PI3K, AKT and p-AKT as well as anti-rabbit or anti-mouse immunoglobulin G as secondary antibodies, were purchased from Cell Signaling Technology, Inc. (Boston, MA, USA). ELISA kit for measurement of serum insulin was purchased from EMD Millipore Corporation, Billerica (San Diego, MA, USA). Rat thiredoxin reductase was obtained from Sigma (St. Louis, MO, USA). Other chemicals were of the highest grade available.

5.2. Preparation of EGCG autoxidation products

EGCG was dissolved in 0.2 M PBS (pH 8.0) at a concentration of 5 mg/mL and was pipetted into 12 \times 100 mm glass tubes (1 mL/tube). Autoxidation of EGCG was allowed at 37 $^{\circ}$ C for 16 or 64 h. Resultant EAOP were rapidly stored at -80° C.

5.3. Fractionation of E64 by ultrafiltration centrifugation

E64 was added to 50 kDa cutoff device (Millipore's Amicon® Ultra-4). The filtrated liquid was collected following centrifugation at 4,000 g (40 min). The procedure was repeated by adding deionized water until the filtrated liquid was colorless. The intercepted liquid was collected as the >50 kDa fraction, and the filtrated liquid was added to 10 kDa cutoff device (Millipore's Amicon® Ultra-4) for repeated centrifugation separation. The resultant filtrated liquid and intercepted liquid were collected as the <10 kDa fraction and the 10–50 kDa fraction, respectively. Each fraction was freeze-dried and stored at -80°C .

5.4. Animal treatments

Male C57BL/KsJ-db/db mice (six weeks of age, 35–40 g) were purchased from Shanghai SLAC Laboratory Animal Co. Ltd (Shanghai, China). They were housed in standard animal cages and maintained in an animal room with the controlled humidity (55–60%), temperature ($23 \pm 2^{\circ}\text{C}$), and the 12-h light/dark cycle. Mice were allowed access to standard laboratory chow and water *ad libitum*. All animal studies (including the mice euthanasia procedure) were done in compliance with the regulations and guidelines of Anhui Agricultural University institutional animal care and conducted according to the AAALAC and the IACUC guidelines (protocol AHOU2019029).

To examine the anti-hyperglycemia effect of various EAOP, db/db mice were randomly divided into four groups ($n = 6/\text{each}$) and were i.p. injected daily with PBS (control group), E0, E16, or E64, respectively, at the dose of 10 mg/kg for 3 consecutive weeks.

To examine the anti-hyperglycemia effect of high-dose E16, db/db mice were randomly divided into two groups ($n = 6/\text{each}$). The control group was i.p. injected once a day with PBS, while the treatment group received E16 at the dose of 40 mg/kg once a day for 4 consecutive days.

To examine the anti-hyperglycemia effect of low-dose E64, db/db mice were randomly divided into three groups ($n = 6/\text{each}$). The control group was i.p. injected once a day with PBS, while the treatment groups received E64 at the dose of 5 or 10 mg/kg for 3 consecutive weeks.

To examine the anti-hyperglycemia effect of different molecular weight fractions of E64, db/db mice were randomly divided into four groups ($n = 6/\text{each}$). The control group was i.p. injected once a day with PBS, while the treatment groups received <10 kDa, 10–50 kDa or >50 kDa fraction of E64, respectively, at the dose of 5 mg/kg for 4 consecutive weeks.

Food intake, water intake, and urine output were measured daily. The blood glucose levels were monitored weekly following 12-h fasting at night.

5.5. ITT

At the end of animal experiment 3, db/db mice were fasted for 12 h, and then i.p. injected with insulin (2 U/kg). Blood glucose levels at 0, 30, 60, 90, and 120 min were measured by ACCU-CHEK Performa (Roche, Basel, Switzerland).

5.6. Sample preparation

At the end of each experiment, all db/db mice were sacrificed by cervical dislocation. Peripheral blood from the ophthalmic vein was collected into an Eppendorf tube, and serum was prepared after coagulation by centrifugation at 10,000 rpm for 10 min and stored at -80°C . Glucose was determined by the oxidase method using a commercial kit from Huili Biotech Co., Ltd (Changchun, Jilin, China). Serum insulin levels were measured using the ELISA kit indicated above. Insulin-responsive tissues (the liver, kidney, skeletal muscle, and adipose tissue) and the pancreatic islet responsible for insulin synthesis were excised and rinsed in ice-cold saline and then stored at -80°C .

The ACE activity was determined via the cleavage of a synthetic

substrate (Abz-based peptide) to release fluorophore Abz, quantified by a fluorescence microplate reader at an excitation wavelength of 330 nm and an emission wavelength of 430 nm. The activity was expressed as mU/mg protein. One mU of ACE activity was defined as pmols of Abz/min/mg protein at 37°C . Similarly, ACE2 activity was determined via the cleavage of a synthetic substrate (MCA-based peptide) to release fluorophore MCA, quantified by a fluorescence microplate reader at an excitation wavelength of 320 nm and an emission wavelength of 420 nm. The activity was expressed as mU/mg protein. One mU of ACE2 activity was defined as pmols of MCA/min/mg protein at room temperature.

5.7. Serum biomarkers

Serum alanine aminotransferase (ALT) and aspartate aminotransferase (AST) activities, as well as serum creatinine (Cr) and blood urea nitrogen (BUN) levels, were measured using commercial kits (Jiancheng Bioengineering Institute, Nanjing, China).

5.8. Liver biomarkers

The liver homogenate was prepared in ice-cold 150 mM PBS (pH 7.2) containing 1 mM EDTANA2 and centrifuged for 15 min at 15,000 g at 4°C . Protein levels were determined by a bicinchoninic acid protein assay kit. Assay for Trx activity was essentially identical to a previous report [39,71], and the activity was expressed as mU/mg protein. One mU of Trx activity was defined as nmols of NADPH oxidized/min/mg protein at 37°C . GPx activity was measured following the method of Smith and Levander [72], and the activity was expressed as U/mg protein. One U of GPx activity was defined as μmols of NADPH oxidized/min/mg protein at 37°C .

5.9. ROS and hydroxyl radical detection

ROS production from the redox system of sodium selenite and glutathione was carried out in 50 mM PBS (pH 7.5) containing 1 mM EDTANA2 at 37°C in the presence of 20 μM sodium selenite, 2 mM glutathione, and 50 μM 2,7-dichlorofluorescein diacetate (DCFH-DA). The fluorescence intensity of the DCFH-DA oxidation product was detected at an excitation wavelength of 488 nm and an emission wavelength of 525 nm in a microplate reader. Hydroxyl radical production from the redox system of copper sulfate and glutathione was carried out in 50 mM PBS (pH 7.5) containing 1 mM EDTANA2 at 37°C in the presence of 10 μM copper sulfate, 30 mM glutathione and 3 mM coumarin-3-carboxylic acid (3-CCA). The fluorescence intensity of the 3-CCA oxidation product was detected at an excitation wavelength of 366 nm and an emission wavelength of 446 nm in a microplate reader.

5.10. Western blot

Samples were boiled with $2 \times$ SDS-PAGE loading buffer and subjected to 12% SDS-PAGE gels separation. Then, the gels were transferred to PVDF membranes. The membranes were then blocked with 5% nonfat dried milk in TBS-T (10 mM Tris-HCl, pH7.8, 150 mM NaCl and 0.05% Tween-20) for 2 h at room temperature. After 5 min wash with TBS-T, the membranes were incubated with primary antibody, which was diluted in TBS-T by 1,000-fold to 10,000-fold at -4°C overnight. The membranes were washed three times with TBS-T (10 min per washing) and then incubated for 2 h at room temperature with a secondary antibody, which was diluted in TBS-T by 5,000-fold. The membranes were washed three times with TBS-T (10 min per washing). Proteins were detected using ChemiDoc XRS + detection system (ECL; Bio-Rad). The Quantity One Image Analyzer software program (Bio-Rad) was used for quantitative densitometric analysis.

5.11. Cell culture

HK-2 cells were cultured in DMEM/F12 (1:1) medium containing 1% (v/v) penicillin and streptomycin and 10% (v/v) fetal bovine serum in a humidified atmosphere containing 5%CO₂/95% air at 37 °C. At 70–80% confluence, cells were cultured in a serum-free medium for 24 h. Then the cells were then treated with 30 µg/mL cholesterol plus 1 µg/mL 25-hydroxycholesterol for 24 h, in the presence or absence of the >50 kDa fraction.

HepG2 cells were cultured in RPMI 1640 medium containing 10% (v/v) fetal bovine serum, 1% (v/v) penicillin and streptomycin, and 1% (v/v) L-glutamine in a humidified atmosphere containing 5%CO₂/95% air at 37 °C. MTT cytotoxicity evaluation was performed as previously described [73].

5.12. MALDI-TOF-MS instrumentation analysis

Mass spectra with *m/z* range from 100 to 50,000 were recorded on UltrafleXtreme MALDI-TOF/TOF instrument (Bruker). One microliter of the >50 kDa fraction from E64 (2.5 µg/mL) was dropped onto the surface of the MALDI target, followed by mixing with an equal volume of saturated HCCA (a matrix for polyphenols analysis) in 50% acetonitrile (v/v, with 0.1% trifluoroacetic acid). After evaporation of the solvent, the probe was introduced into the ion source, and the compounds were ionized by laser energy. External calibration was performed with the peptide calibration standards supplied from Bruker. Tannic acid was used as a positive reference. The mass spectra were obtained from the recorded raw data using Flexi Analysis software.

5.13. Statistical analysis

All statistical analyses were performed using the Prism version 5 software (GraphPad, San Diego, CA, USA). The data were presented as means ± SEM (standard error of mean). Significant differences among groups were examined by Student's *t*-test, Mann Whitney test, or one-way analysis of variance post hoc Tukey's or Dunnett's test as appropriate. A *P* value < 0.05 was considered statistically significant.

Funding

This work was supported by the National Natural Science Foundation of China (Grant numbers: 31771971).

Author contributions

J.Z. conceived the study and designed the experiments. X.W., M.Y., Y.H., F.W., and Y.K. performed the experiments. J.Z. X.W., M.Y., and T.L. analyzed the data. J.Z. and X.W. prepared the manuscript.

Declaration of competing interest

The authors have no competing or conflicting interests to declare.

Appendix A. Supplementary data

Supplementary data to this article can be found online at <https://doi.org/10.1016/j.redox.2022.102259>.

References

- [1] M.T. Zanella, O. Kohlmann, A.B. Ribeiro, Treatment of obesity hypertension and diabetes syndrome, *Hypertension* 38 (3 Pt 2) (2001) 705–708.
- [2] G.M. Reaven, Banting lecture 1988. Role of insulin resistance in human disease, *Diabetes* 37 (12) (1988) 1595–1607.
- [3] J.M. Luther, N.J. Brown, The renin-angiotensin-aldosterone system and glucose homeostasis, *Trends Pharmacol. Sci.* 32 (12) (2011) 734–739.
- [4] K. Putnam, R. Shoemaker, F. Yiannikouris, L.A. Cassis, The renin-angiotensin system: a target of and contributor to dyslipidemias, altered glucose homeostasis, and hypertension of the metabolic syndrome, *Am. J. Physiol. Heart Circ. Physiol.* 302 (6) (2012) H1219–H1230.
- [5] T. Shiuchi, M. Iwai, H.-S. Li, L. Wu, L.-J. Min, J.-M. Li, et al., Angiotensin II type-1 receptor blocker valsartan enhances insulin sensitivity in skeletal muscles of diabetic mice, *Hypertension* 43 (5) (2004) 1003–1010.
- [6] G.A. Favre, V.L.M. Esnault, E. Van Obberghen, Modulation of glucose metabolism by the renin-angiotensin-aldosterone system, *Am. J. Physiol. Endocrinol. Metab.* 308 (6) (2015) E435–E449.
- [7] M.C. Blendea, D. Jacobs, C.S. Stump, S.I. McFarlane, C. Ogrin, G. Bahtiyar, et al., Abrogation of oxidative stress improves insulin sensitivity in the Ren-2 rat model of tissue angiotensin II overexpression, *Am. J. Physiol. Endocrinol. Metab.* 288 (2) (2005) E353–E359.
- [8] G. Lastra, J. Habibi, A.T. Whaley-Connell, C. Manrique, M.R. Hayden, J. Rehmer, et al., Direct renin inhibition improves systemic insulin resistance and skeletal muscle glucose transport in a transgenic rodent model of tissue renin overexpression, *Endocrinology* 150 (6) (2009) 2561–2568.
- [9] J.M. Perkins, S.N. Davis, The renin-angiotensin-aldosterone system: a pivotal role in insulin sensitivity and glycemic control, *Curr. Opin. Endocrinol. Diabetes Obes.* 15 (2) (2008) 147–152.
- [10] H. Misu, T. Takamura, H. Takayama, H. Hayashi, N. Matsuzawa-Nagata, S. Kurita, et al., A liver-derived secretory protein, selenoprotein P, causes insulin resistance, *Cell Metabol.* 12 (5) (2010) 483–495.
- [11] H. Takayama, H. Misu, H. Iwama, K. Chikamoto, Y. Saito, K. Muraio, et al., Metformin suppresses expression of the selenoprotein P gene via an AMP-activated kinase (AMPK)/FoxO3a pathway in H4IIEC3 hepatocytes, *J. Biol. Chem.* 289 (1) (2014) 335–345.
- [12] K. Ishikura, H. Misu, M. Kumazaki, H. Takayama, N. Matsuzawa-Nagata, N. Tajima, et al., Selenoprotein P as a diabetes-associated hepatokine that impairs angiogenesis by inducing VEGF resistance in vascular endothelial cells, *Diabetologia* 57 (9) (2014) 1968–1976.
- [13] B. Speckmann, H. Sies, H. Steinbrenner, Attenuation of hepatic expression and secretion of selenoprotein P by metformin, *Biochem. Biophys. Res. Commun.* 387 (1) (2009) 158–163.
- [14] Y. Mita, K. Nakayama, S. Inari, Y. Nishito, Y. Yoshioka, N. Sakai, et al., Selenoprotein P-neutralizing antibodies improve insulin secretion and glucose sensitivity in type 2 diabetes mouse models, *Nat. Commun.* 8 (1) (2017) 1658.
- [15] N.M. Alhawiti, S. Al Mahri, M.A. Aziz, S.S. Malik, S. Mohammad, TXNIP in metabolic regulation: physiological role and therapeutic outlook, *Curr. Drug Targets* 18 (9) (2017) 1095–1103.
- [16] L. Thielen, A. Shalev, Diabetes pathogenic mechanisms and potential new therapies based upon a novel target called TXNIP, *Curr. Opin. Endocrinol. Diabetes Obes.* 25 (2) (2018) 75–80.
- [17] A. Shah, L. Xia, E.A.Y. Masson, C. Gui, A. Momen, E.A. Shikatani, et al., Thioredoxin-interacting protein deficiency protects against diabetic nephropathy, *J. Am. Soc. Nephrol.* 26 (12) (2015) 2963–2977.
- [18] A. Kumar, R. Mittal, Mapping Txnip: key connexions in progression of diabetic nephropathy, *Pharmacol. Rep.* 70 (3) (2018) 614–622.
- [19] H.-S. Kim, M.J. Quon, J.-A. Kim, New insights into the mechanisms of polyphenols beyond antioxidant properties; lessons from the green tea polyphenol, epigallocatechin 3-gallate, *Redox Biol.* 2 (2014) 187–195.
- [20] C.S. Yang, J. Zhang, L. Zhang, J. Huang, Y. Wang, Mechanisms of body weight reduction and metabolic syndrome alleviation by tea, *Mol. Nutr. Food Res.* 60 (1) (2016) 160–174.
- [21] H. Cao, I. Hininger-Favie, M.A. Kelly, R. Benaraba, H.D. Dawson, S. Coves, et al., Green tea polyphenol extract regulates the expression of genes involved in glucose uptake and insulin signaling in rats fed a high fructose diet, *J. Agric. Food Chem.* 55 (15) (2007) 6372–6378.
- [22] L.-Y. Wu, C.-C. Juan, L.S. Hwang, Y.-P. Hsu, P.-H. Ho, L.-T. Ho, Green tea supplementation ameliorates insulin resistance and increases glucose transporter IV content in a fructose-fed rat model, *Eur. J. Nutr.* 43 (2) (2004) 116–124.
- [23] Y.-K. Chen, C. Cheung, K.R. Reuhl, A.B. Liu, M.-J. Lee, Y.-P. Lu, et al., Effects of green tea polyphenol (-)-epigallocatechin-3-gallate on newly developed high-fat/Western-style diet-induced obesity and metabolic syndrome in mice, *J. Agric. Food Chem.* 59 (21) (2011) 11862–11871.
- [24] M. Bose, J.D. Lambert, J. Ju, K.R. Reuhl, S.A. Shapses, C.S. Yang, The major green tea polyphenol, (-)-epigallocatechin-3-gallate, inhibits obesity, metabolic syndrome, and fatty liver disease in high-fat-fed mice, *J. Nutr.* 138 (9) (2008) 1677–1683.
- [25] H. Ortsäter, N. Grankvist, S. Wolfram, N. Kuehn, A. Sjöholm, Diet supplementation with green tea extract epigallocatechin gallate prevents progression to glucose intolerance in db/db mice, *Nutr. Metab.* 9 (2012) 11.
- [26] S. Wolfram, D. Raederstorff, M. Preller, Y. Wang, S.R. Teixeira, C. Riegger, et al., Epigallocatechin gallate supplementation alleviates diabetes in rodents, *J. Nutr.* 136 (10) (2006) 2512–2518.
- [27] S. Sang, M.-J. Lee, Z. Hou, C.-T. Ho, C.S. Yang, Stability of tea polyphenol (-)-epigallocatechin-3-gallate and formation of dimers and epimers under common experimental conditions, *J. Agric. Food Chem.* 53 (24) (2005) 9478–9484.
- [28] G.H. Yassin, J.H. Koek, N. Kuhnert, Model system-based mechanistic studies of black tea thearubigin formation, *Food Chem.* 180 (2015) 272–279.
- [29] M.-P. Gonthier, J.L. Donovan, O. Texier, C. Felgines, C. Remy, A. Scalbert, Metabolism of dietary procyanidins in rats, *Free Radic. Biol. Med.* 35 (8) (2003) 837–844.

- [30] C. Manach, G. Williamson, C. Morand, A. Scalbert, C. Rémésy, Bioavailability and bioefficacy of polyphenols in humans. I. Review of 97 bioavailability studies, *Am. J. Clin. Nutr.* 81 (1 Suppl) (2005) 230S–242S.
- [31] Y. Wei, P. Chen, T. Ling, Y. Wang, R. Dong, C. Zhang, et al., Certain (-)-epigallocatechin-3-gallate (EGCG) auto-oxidation products (EAOPs) retain the cytotoxic activities of EGCG, *Food Chem.* 204 (2016) 218–226.
- [32] T.-T. An, S. Feng, C.-M. Zeng, Oxidized epigallocatechin gallate inhibited lysozyme fibrillation more strongly than the native form, *Redox Biol.* 11 (2017) 315–321.
- [33] L. Zhou, F. Wu, W. Jin, B. Yan, X. Chen, Y. He, et al., Theabrownin inhibits cell cycle progression and tumor growth of lung carcinoma through c-myc-related mechanism, *Front. Pharmacol.* 8 (2017) 75.
- [34] J.I. Ottaviani, L. Actis-Goretta, J.J. Villordo, C.G. Fraga, Procyanidin structure defines the extent and specificity of angiotensin I converting enzyme inhibition, *Biochimie* 88 (2006) 359–365.
- [35] L. Actis-Goretta, J.I. Ottaviani, C.L. Keen, C.G. Fraga, Inhibition of angiotensin converting enzyme (ACE) activity by flavan-3-ols and procyanidins, *FEBS Lett.* 555 (2003) 597–600.
- [36] R. Pierini, P.A. Kroon, S. Guyot, K. Ivory, I.T. Johnson, N.J. Belshaw, Procyanidin effects on oesophageal adenocarcinoma cells strongly depend on flavan-3-ol degree of polymerization, *Mol. Nutr. Food Res.* 52 (2008) 1399–1407.
- [37] H.C. Gerstein, H.M. Colhoun, G.R. Dagenais, R. Diaz, M. Lakshmanan, P. Pais, et al., Dulaglutide and cardiovascular outcomes in type 2 diabetes (REWIND): a double-blind, randomised placebo-controlled trial, *Lancet* 394 (10193) (2019) 121–130.
- [38] D.L. Hay, S. Chen, T.A. Lutz, D.G. Parkes, J.D. Roth, Amylin: pharmacology, physiology, and clinical potential, *Pharmacol. Rev.* 67 (3) (2015) 564–600.
- [39] G. Zhao, X. Wu, P. Chen, L. Zhang, C.S. Yang, J. Zhang, Selenium nanoparticles are more efficient than sodium selenite in producing reactive oxygen species and hyper-accumulation of selenium nanoparticles in cancer cells generates potent therapeutic effects, *Free Radic. Biol. Med.* 126 (2018) 55–66.
- [40] K. Ngamchuea, C. Batchelor-McAuley, R.G. Compton, The copper(II)-Catalyzed oxidation of glutathione, *Chemistry* 22 (44) (2016) 15937–15944.
- [41] C. Meyer, M. Stumvoll, V. Nadkarni, J. Dostou, A. Mitrakou, J. Gerich, Abnormal renal and hepatic glucose metabolism in type 2 diabetes mellitus, *J. Clin. Invest.* 102 (3) (1998) 619–624.
- [42] A. Mitrakou, Kidney: its impact on glucose homeostasis and hormonal regulation, *Diabetes Res. Clin. Pract.* 93 (Suppl 1) (2011) S66–S72.
- [43] Y. Wu, K.L. Ma, Y. Zhang, Y. Wen, G.H. Wang, Z.B. Hu, et al., Lipid disorder and intrahepatic renin-angiotensin system activation synergistically contribute to non-alcoholic fatty liver disease, *Liver Int.* 36 (10) (2016) 1525–1534.
- [44] K.-L. Ma, J. Ni, C.-X. Wang, J. Liu, Y. Zhang, Y. Wu, et al., Interaction of RAS activation and lipid disorders accelerates the progression of glomerulosclerosis, *Int. J. Med. Sci.* 10 (12) (2013) 1615–1624.
- [45] E. Haslam, Thoughts on thearubigins, *Phytochemistry* 64 (1) (2003) 61–73.
- [46] M.-C. Menet, S. Sang, C.S. Yang, C.-T. Ho, R.T. Rosen, Analysis of theaflavins and thearubigins from black tea extract by MALDI-TOF mass spectrometry, *J. Agric. Food Chem.* 52 (9) (2004) 2455–2461.
- [47] N. Kuhnert, Unraveling the structure of the black tea thearubigins, *Arch. Biochem. Biophys.* 501 (1) (2010) 37–51.
- [48] A. Supersaxo, W.R. Hein, H. Steffen, Effect of molecular weight on the lymphatic absorption of water-soluble compounds following subcutaneous administration, *Pharm. Res. (N. Y.)* 7 (2) (1990) 167–169.
- [49] V. Kozlovskaya, O. Zavgorodnya, Y. Chen, K. Ellis, H.M. Tse, W. Cui, et al., Ultrathin polymeric coatings based on hydrogen-bonded polyphenol for protection of pancreatic islet cells, *Adv. Funct. Mater.* 22 (16) (2012) 3389–3398.
- [50] J.M. Barra, V. Kozlovskaya, E. Kharlampieva, H.M. Tse, Localized immunosuppression with tannic acid encapsulation delays islet allograft and autoimmune-mediated rejection, *Diabetes* 69 (9) (2020) 1948–1960.
- [51] Z. Yan, H.R. Spaulding, Extracellular superoxide dismutase, a molecular transducer of health benefits of exercise, *Redox Biol.* 32 (2020) 101508.
- [52] K. Mohammadi, N. Bellili-Muñoz, S.L. Marklund, F. Driss, H. Le Nagard, T. A. Patente, et al., Plasma extracellular superoxide dismutase concentration, allelic variations in the SOD3 gene and risk of myocardial infarction and all-cause mortality in people with type 1 and type 2 diabetes, *Cardiovasc. Diabetol.* 14 (2015) 845.
- [53] G. Feng, J.-L. Gao, P. Zhang, J.-J. Huang, L.-Z. Huang, L. Cheng, et al., Decreased serum extracellular superoxide dismutase activity is associated with albuminuria in Chinese patients with type 2 diabetes mellitus, *Acta Diabetol.* 54 (11) (2017) 1047–1055.
- [54] H. Fujita, H. Fujishima, S. Chida, K. Takahashi, Z. Qi, Y. Kanetsuna, et al., Reduction of renal superoxide dismutase in progressive diabetic nephropathy, *J. Am. Soc. Nephrol.* 20 (6) (2009) 1303–1313.
- [55] T. Fukai, R.J. Folz, U. Landmesser, D.G. Harrison, Extracellular superoxide dismutase and cardiovascular disease, *Cardiovasc. Res.* 55 (2) (2002) 239–249.
- [56] J.-S. Zhao, H.-X. Jin, J.-L. Gao, C. Pu, P. Zhang, J.-J. Huang, et al., Serum extracellular superoxide dismutase is associated with diabetic retinopathy stage in Chinese patients with type 2 diabetes mellitus, *Dis. Markers* 2018 (2018) 8721379.
- [57] J.-Q. Huang, J.-C. Zhou, Y.-Y. Wu, F.-Z. Ren, X.G. Lei, Role of glutathione peroxidase 1 in glucose and lipid metabolism-related diseases, *Free Radic. Biol. Med.* 127 (2018) 108–115.
- [58] J.P. McClung, C.A. Roneker, W. Mu, D.J. Lisk, P. Langlais, F. Liu, et al., Development of insulin resistance and obesity in mice overexpressing cellular glutathione peroxidase, *Proc. Natl. Acad. Sci. U. S. A.* 101 (24) (2004) 8852–8857.
- [59] Y. Wei, J.R. Sowers, R. Nistala, H. Gong, G.M.E. Uptergrove, S.E. Clark, et al., Angiotensin II-induced NADPH oxidase activation impairs insulin signaling in skeletal muscle cells, *J. Biol. Chem.* 281 (46) (2006) 35137–35146.
- [60] M.H. Lee, H.K. Song, G.J. Ko, Y.S. Kang, S.Y. Han, K.H. Han, et al., Angiotensin receptor blockers improve insulin resistance in type 2 diabetic rats by modulating adipose tissue, *Kidney Int.* 74 (7) (2008) 890–900.
- [61] S.J. Fletcher, N.S. Kalupahana, M. Soltani-Bejnood, J.H. Kim, A.M. Saxton, D. H. Wasserman, et al., Transgenic mice overexpressing Renin exhibit glucose intolerance and diet-genotype interactions, *Front. Endocrinol.* 3 (2012) 166.
- [62] P. Chan, K.-L. Wong, I.M. Liu, T.-F. Tzeng, T.-L. Yang, J.-T. Cheng, Antihyperglycemic action of angiotensin II receptor antagonist, valsartan, in streptozotocin-induced diabetic rats, *J. Hypertens.* 21 (4) (2003) 761–769.
- [63] B.M. Brenner, M.E. Cooper, D. de Zeeuw, W.F. Keane, W.E. Mitch, H.H. Parving, et al., Effects of losartan on renal and cardiovascular outcomes in patients with type 2 diabetes and nephropathy, *N. Engl. J. Med.* 345 (12) (2001) 861–869.
- [64] H.H. Parving, H. Lehnert, J. Bröchner-Mortensen, R. Gomis, S. Andersen, P. Arner, The effect of irbesartan on the development of diabetic nephropathy in patients with type 2 diabetes, *N. Engl. J. Med.* 345 (12) (2001) 870–878.
- [65] A. Sahr, C. Wolke, J. Maczewsky, P. Krippeit-Drews, A. Tetzner, G. Drews, et al., The angiotensin-(1-7)/mas Axis improves pancreatic β -cell function in vitro and in vivo, *Endocrinology* 157 (12) (2016) 4677–46790.
- [66] R. Shoemaker, F. Yiannikouris, S. Thatcher, L. Cassis, ACE2 deficiency reduces β -cell mass and impairs β -cell proliferation in obese C57BL/6 mice, *Am. J. Physiol. Endocrinol. Metab.* 309 (7) (2015) E621–E631.
- [67] P.S. Leung, Mechanisms of protective effects induced by blockade of the renin-angiotensin system: novel role of the pancreatic islet angiotensin-generating system in Type 2 diabetes, *Diabet. Med.* 24 (2) (2007) 110–116.
- [68] M.R. Hayden, J.R. Sowers, Isletopathy in Type 2 diabetes mellitus: implications of islet RAS, islet fibrosis, islet amyloid, remodeling, and oxidative stress, *Antioxidants Redox Signal.* 9 (7) (2007) 891–910.
- [69] A. Shalev, Minireview: thioredoxin-interacting protein: regulation and function in the pancreatic β -cell, *Mol. Endocrinol.* 28 (8) (2014) 1211–1220.
- [70] A.H. Minn, C. Hafele, A. Shalev, Thioredoxin-interacting protein is stimulated by glucose through a carbohydrate response element and induces beta-cell apoptosis, *Endocrinology* 146 (5) (2005) 2397–2405.
- [71] X. Wu, G. Zhao, Y. He, W. Wang, C.S. Yang, J. Zhang, Pharmacological mechanisms of the anticancer action of sodium selenite against peritoneal cancer in mice, *Pharmacol. Res.* 147 (2019) 104360.
- [72] A.D. Smith, C.A. Guidry, V.C. Morris, O.A. Levander, Aurothioglucose inhibits murine thioredoxin reductase activity in vivo, *J. Nutr.* 129 (1) (1999) 194–198.
- [73] L. Zhang, Y. He, X. Wu, G. Zhao, K. Zhang, C.S. Yang, et al., Melatonin and (-)-Epigallocatechin-3-Gallate: partners in fighting cancer, *Cells* 8 (7) (2019).